

# “Quantum phase transitions” in classical nonequilibrium processes

Oded Agam and Nadav M. Shnerb<sup>a</sup>

<sup>a</sup>Department of Physics, The Hebrew University, Jerusalem, Israel 91904

## Abstract

Diffusion limited reaction of the Lotka-Volterra type is analyzed taking into account the discrete nature of the reactants. In the continuum approximation, the dynamics is dominated by an elliptic fixed-point over the whole parameter space of the system. Discretization effects break the parameter space into several phases where the system exhibits a distinct behavior: The fixed-point becomes either stable (node or focus) or unstable (node or focus). The results are verified by extensive numerical simulations. These simulations also suggest that, in the unstable phase, a new ground state is formed, where the dynamics flows into a limit cycle.

*PACS:* 82.40.Bj 05.45.Ac 82.20.Mj 87.23.Cc

*Keywords:* Lotka-Volterra equations, Quantization, Renormalization

## 1. Introduction

Nonequilibrium systems of diffusing reactants are very common in nature. In chemistry almost any chemical reaction is a reaction-diffusion system. In physics, the standard examples are annihilation of electrons and holes moving in a disordered media, or vortices and antivortices in type two superconductors. Examples from other fields include: population dynamics in biology, spread of epidemics in health science, and group decision dynamics in social science.

It is customary to denote the various types of reactants by capital letters,  $A$ ,  $B$ ,  $C$ , etc., and the rates of the reactions by Greek letters  $\mu$ ,  $\lambda$ ,  $\sigma$ , etc. Then, for example, a process in which  $A$  and  $B$  annihilate each other at rate  $\lambda$  is represented symbolically as:  $A + B \xrightarrow{\lambda} \emptyset$ . Similarly, a process where the reaction of  $A$  and  $B$  produces  $C$ , at rate  $\mu$ , is represented by  $A + B \xrightarrow{\mu} C$ .

The simplest description of reaction-diffusion dynamics employs the densities of the reactants as the basic ingredients of the equations of motion. For example, the equation describing the binary annihilation reaction



is

$$\frac{\partial n_A}{\partial t} = D \nabla^2 n_A - \mu n_A^2, \quad (2)$$

where  $n_A$  is the density of the reactants, and  $D$  is their diffusion constant. The first term in the above equation represents the diffusive behavior of the particles, while the second term accounts for the interaction. We shall call these kind of equations “mean field equations” for reasons which will be clarified later on.

The evolution of many nonequilibrium processes are adequately described by mean field equations. One of the most remarkable examples is the Belousov-Zhabotinskii reaction [1] where a mixture of few chemical reactants produces a nonequilibrium process which is periodic in time.

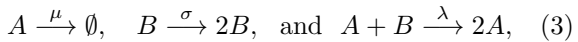
Facing the success of the mean field theory, it is natural to ask whether, indeed, it always gives an accurate description of reaction-diffusion systems. In fact, it is known that the answer for this question is negative. Deviations from the mean field theory appear, usually, in systems of low dimensionality. Returning to the example (1), it can be easily seen that the homogeneous solution of equation (2) behaves asymptotically as  $n_A \sim 1/t$ , independent of the dimensionality of the system. However, the true asymptotic behavior of (1) is  $n_A \sim 1/\sqrt{t}$  in 1d,  $n_A \sim \ln t/t$  in

$2d$ , and  $n_A \sim 1/t$ , for  $d > 2$  [2].

$d = 2$  is the critical dimension for reaction-diffusion type of nonequilibrium processes. The qualitative explanation for this behavior is clear: In order to react, the two particles should first diffuse to make contact. This diffusion time restricts the rate of the reaction since, in low dimensions, diffusion is inefficient in mixing the reactants. The Ovchinnikov-Zeldovich segregation phenomenon[3] is the result of spatially inactive regions developed in diffusion limited reactions.

The purpose of this work is to present an example for nonequilibrium process in which the discretized nature of the reactants has a strong impact on the behavior: The mean field equations completely fail to describe the dynamics of the system in the long time limit. The parameter space, spanned by the reaction rates  $(\mu, \sigma, \dots)$ , breaks into subspaces where the system exhibits a distinct behavior, and the transition from one subspace to another is analogous to a quantum phase transition.

The prototype example we shall use is one of the simplest models of population biology: the Lotka-Volterra system [4,5]. In the predator-prey version of this model, two species, a predator (A) and a prey (B) are interacting while all other environmental factors are assumed intact. In the absence of predator, the prey population grows exponentially, while in the absence of prey the predator death rate results in an exponential decay of their population. Binary interaction between the species involves the growth of the predator population due to consumption of the prey, thus:



where  $\mu$  is the predator death rate,  $\sigma$  is the prey birth rate, and  $\lambda$  is the probability for a predator to eat a prey at the same spatial location. We assume that birth of a new predator follows an “eating event” at the same site. The mean field equations of this system are the Lotka-Volterra equations:

$$\begin{aligned} \frac{dn_A}{dt} &= D\nabla^2 n_A - \mu n_A + \lambda n_A n_B, \\ \frac{dn_B}{dt} &= D\nabla^2 n_B + \sigma n_B - \lambda n_A n_B. \end{aligned} \quad (4)$$

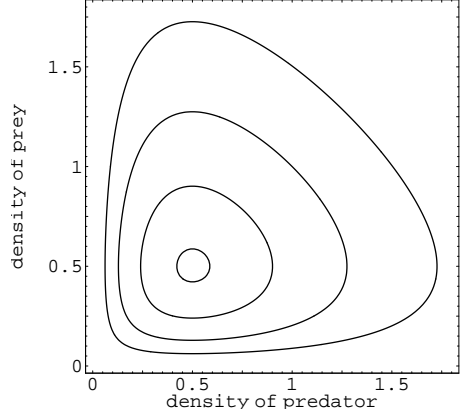


Figure 1. Examples of phase space trajectories corresponding to the homogeneous solution of the mean field equations (4).

Here  $n_A$  and  $n_B$  denote the population densities of the predator and prey, respectively, and it is assumed that the diffusion constants of both species equal to  $D$ . The generic behavior of this system is periodic in time, see Fig. 1. When the number prey is large, the predator population is growing due to the availability of food, but then the prey population decreases. Consequently, also the predator population diminishes. When the predator population is already small, the number of prey, again, begins growing and the cycle repeats.

Here, we will show that the behavior of the quantized version of this model, in two dimensions, does not follow the Lotka-Volterra equations (4). Our analysis will proceed in the following way. First, we write down the exact Master equations of the quantized version of the system. Then, we map these equations onto a Schrödinger equation in imaginary time, and identify the corresponding many-body Hamiltonian. Next, we express the propagator of the system as a field integral and find the corresponding action. It will be shown that the mean field equations (4) are the saddle point equations associated with this action. The effective action of the system will be, then, constructed follow-

ing the traditional procedure of renormalization. Namely, the fields will be separated into “fast” and “slow” components, and the fast components will be integrated out. Finally, we analyze the saddle point equation of the effective action and classify the system behavior in various regimes of the parameter space  $(\mu, \sigma, \lambda)$ . Our results will be verified by numerical simulations.

To avoid cumbersome algebraic manipulations, our discussion will be switching between two processes: the binary annihilation (1), and the Lotka-Volterra reaction (3). The first example will be used as a simple illustration of the derivation, while the results for the Lotka-Volterra reaction will be usually stated without an explicit derivation.

## 2. The Master Equations

The Master equations of a nonequilibrium process are equations for the probabilities of the various states of the system. Consider the binary annihilation process (1) in zero dimension, i.e. when the system consists of a single site. Then, a state of the system is defined by the number of reactants,  $n$ , and we denote the probability to find the system in this state by  $P_n$ . The Master equations relate the change of probability in time to the rate of flow into and out of the state:

$$\frac{dP_n}{dt} = -\frac{\mu}{2} [n(n-1)P_n - (n+2)(n+1)P_{n+2}]. \quad (5)$$

The first term on the right hand side represents the flow out of the state with  $n$  reactants. It comes from pair annihilation, and therefore proportional to the number of pairs,  $n(n-1)/2$ . The second term accounts for the flow into the state which is due to pair annihilation in the state with  $n+2$  reactants.

The same logic can be used in order to construct the Master equations for the Lotka-Volterra process (3). Considering again the zero dimensional case, they take the form

$$\begin{aligned} \frac{dP_{m,n}}{dt} = & -(\mu m + \sigma n + \lambda mn)P_{m,n} & (6) \\ & + \mu(m+1)P_{m+1,n} + \sigma(n-1)P_{m,n-1} \\ & + \lambda(m-1)(n+1)P_{m-1,n+1}, \end{aligned}$$

where  $P_{m,n}$  denotes the probability to find the system in a state with  $m$  predator and  $n$  prey.

The generalization of the above equations to the non-zero dimensional case is straightforward. A state of the system is now defined by two vectors of integer numbers:  $\mathbf{n} = (n_1, n_2, \dots)$ , and  $\mathbf{m} = (m_1, m_2, \dots)$ . The components of these vectors represent the occupation numbers of the prey and the predator at the various sites of the system, and  $P_{\mathbf{m},\mathbf{n}}$  is the joint probability of the occupation configurations. The Master equations, in this case, contain an additional hopping term between the sites. This term will be added to our theory later on.

## 3. Mapping the Master equations onto a Schrödinger equation

We turn now to map the Master equations onto the Schrödinger equation in imaginary time, and to identify the corresponding many-body Hamiltonian. Beginning with the example of binary annihilation process in zero dimensions, following Refs. [6,7], we define the wave function

$$|\psi\rangle = \sum_{n=0}^{\infty} P_n |n\rangle, \quad (7)$$

where  $|n\rangle$  denotes a state with  $n$  reactants in the system. Taking the derivative of  $|\psi\rangle$  with respect to time and substituting (5) we obtain

$$\begin{aligned} \frac{d}{dt}|\psi\rangle = & \sum_n \frac{dP_n}{dt} |n\rangle = & (8) \\ & -\frac{\mu}{2} \sum_n [n(n-1)P_n - (n+2)(n+1)P_{n+2}] |n\rangle. \end{aligned}$$

Let us now introduce the creation,  $\hat{a}^\dagger$ , and annihilation,  $\hat{a}$ , operators which satisfy the Bose commutation relation  $[\hat{a}, \hat{a}^\dagger] = 1$ , and

$$\hat{a}^\dagger |n\rangle = |n+1\rangle, \quad \text{while} \quad \hat{a} |n\rangle = n |n-1\rangle. \quad (9)$$

It is easy to see that  $\hat{a}^2 |\psi\rangle = \sum_n P_{n+2} (n+2)(n+1) |n\rangle$ , and  $(\hat{a}^\dagger)^2 \hat{a}^2 |\psi\rangle = \sum_n P_n (n-1)n |n\rangle$ . Substituting these results in equation (8), one can write it in the form of a Schrödinger equation in imaginary time

$$\frac{d}{dt}|\psi\rangle = -H|\psi\rangle, \quad (10)$$

where the Hamiltonian is given by

$$H = \frac{\mu}{2}(\hat{a}^\dagger \hat{a}^\dagger - 1)\hat{a}\hat{a}. \quad (11)$$

Turning to the Lotka–Volterra reaction in zero dimension, we denote by  $|m, n\rangle$  the state with  $m$  predator and  $n$  prey. The corresponding wave function is  $|\psi\rangle = \sum_{n,m} P_{m,n} |m, n\rangle$ , and the equations of motion take the same form as (10), but with the Hamiltonian:

$$H = \mu(\hat{a}^\dagger - 1)\hat{a} + \sigma(1 - \hat{b}^\dagger)\hat{b}^\dagger \hat{b} + \lambda\hat{a}^\dagger(\hat{b}^\dagger - \hat{a}^\dagger)\hat{a}\hat{b}. \quad (12)$$

Here  $\hat{a}^\dagger$  and  $\hat{a}$  are the creation and annihilation operators of predator, while  $\hat{b}^\dagger$  and  $\hat{b}$  are the creation and annihilation operators of prey.

The generalization of equation (10) to the nonzero dimensional case is obtained by defining the creation and annihilation operators at each site of the system (i.e.  $\hat{a}^\dagger \rightarrow \hat{a}_i^\dagger, \hat{a} \rightarrow \hat{a}_i, \hat{b}^\dagger \rightarrow \hat{b}_i^\dagger, \hat{b} \rightarrow \hat{b}_i$ , with  $[\hat{a}_j, \hat{a}_i^\dagger] = \delta_{ij}$ , etc.), and adding a hopping term to the Hamiltonian. The wave function, in this case, is

$$|\psi\rangle = \sum_{\mathbf{n}, \mathbf{m}} P_{\mathbf{m}, \mathbf{n}} \prod_i (\hat{a}_i^\dagger)^{m_i} (\hat{b}_i^\dagger)^{n_i} |0\rangle,$$

where  $m_i$  and  $n_i$  are the components of  $\mathbf{m}$  and  $\mathbf{n}$ , and  $|0\rangle$  denotes the vacuum state with no reactants in the system.

#### 4. The formal solution of the Schrödinger equation, and expectation values

The formal solution of the Schrödinger equation (10) is

$$|\psi(t)\rangle = U(t)|\psi(0)\rangle,$$

where  $\psi(0)$  is the initial wave function, and  $U(t)$  is the propagator of the system for time  $t$ , i.e.

$$U(t) = \mathcal{T} \exp \left\{ - \int_0^t dt' H(t') \right\},$$

$\mathcal{T}$  being the time ordering operator. This solution of  $\psi$ , as function of the time, fully characterize the behavior of the system. Notice, however, that the interpretation of the wave function differs from that of quantum mechanics. Here it represents probability and not probability amplitude. In particular, the expectation value of an

operator,  $\hat{Q}$ , in a state defined by  $\psi$  is given by the matrix element [6,7]

$$\langle \hat{Q} \rangle = \langle \mathcal{P} | \hat{Q} | \psi \rangle \quad (13)$$

where

$$|\mathcal{P}\rangle = \prod_i e^{\hat{a}_i^\dagger + \hat{b}_i^\dagger} |0\rangle,$$

is an eigenstate of the annihilation operators, i.e.

$$\hat{a}_j |\mathcal{P}\rangle = \hat{b}_j |\mathcal{P}\rangle = |\mathcal{P}\rangle \quad \text{for any } j. \quad (14)$$

In understanding the structure of this nonequilibrium theory, it is instructive to consider specific examples of expectation values. Consider, first, the expectation value of the identity operator  $\hat{Q} = 1$ . Using the identity

$$e^{\hat{a}} f(\hat{a}^\dagger, \hat{a}) = f(\hat{a}^\dagger + 1, \hat{a}) e^{\hat{a}}, \quad (15)$$

where  $f(\hat{a}^\dagger, \hat{a})$  is a general function of the creation and annihilation operators, one can easily see that  $\langle \mathcal{P} | \psi \rangle = \sum_{\mathbf{n}, \mathbf{m}} P_{\mathbf{m}, \mathbf{n}}$ . Since the sum of probabilities over all possible occupation configurations equals unity, we obtain  $\langle \hat{Q} \rangle = 1$ . Thus the normalization of the wave function reads  $\langle P | \psi \rangle = 1$ .

The conservation of probability implies that  $\langle P | \psi \rangle = 1$  holds for any time  $t$ , therefore

$$\frac{d}{dt} \langle \mathcal{P} | U(t) | \psi \rangle = 0.$$

This equation is satisfied only if  $\langle \mathcal{P} | H = 0$ . Thus, a legitimate Hamiltonian of our theory must vanish when setting all the creation operators to one. For example, the Lotka–Volterra Hamiltonian should satisfy

$$H(\{\hat{a}_i^\dagger = 1, \hat{b}_i^\dagger = 1, \hat{a}_i, \hat{b}_i\}) = 0.$$

It is easy to verify that (11) and (12), indeed, satisfy this condition.

As a second example, let us calculate the mean number of predator at site  $i$ ,  $\bar{n}_i = \langle \hat{a}_i^\dagger \hat{a}_i \rangle$ . Notice that, unlike quantum mechanics where the expectation value of an annihilation operator vanish, here (14) implies that  $\bar{n}_i = \langle \hat{a}_i \rangle$ . Substituting  $\hat{Q} = \hat{a}_i$  in (13) and using (15) we obtain  $\bar{n}_i = \sum_{\mathbf{n}, \mathbf{m}} n_i P_{\mathbf{n}, \mathbf{m}}$  where  $n_i$  is the number of prey at site  $i$ .

## 5. The field theoretic formalism

In order to construct the propagator,  $U(t)$ , it is convenient to employ the path integral formalism. To begin with, let us consider the propagator of binary annihilation in the zero dimension. We define a coherent state of the system as

$$|a\rangle = e^{-\frac{|a|^2}{2}} e^{a\hat{a}^\dagger} |0\rangle,$$

where  $a$  is a complex number. The matrix element of a normal ordered operator  $f(\hat{a}^\dagger, \hat{a})$ , where all creation operators stand left to annihilation operators, is given by

$$\langle a|f(\hat{a}^\dagger, \hat{a})|a'\rangle = f(a^*, a') e^{-\frac{1}{2}(|a|^2 + |a'|^2 - 2a^*a')}, \quad (16)$$

In particular, the inner product of coherent states is  $\langle a|a'\rangle = \exp\{-\frac{1}{2}(|a|^2 + |a'|^2 - 2a^*a')\}$ , and the normalization condition  $\langle a|a\rangle = 1$  is satisfied. The resolution of identity associated with coherent states is

$$\int \frac{d^2a}{\pi} |a\rangle\langle a|, \quad (17)$$

where  $d^2a = d\Re a \, d\Im a$ .

Consider the expectation value of a general operator  $\hat{Q} = Q(\hat{a}^\dagger, \hat{a})$  at time  $t$ ,

$$\langle \hat{Q}(t) \rangle = \langle P|Q(\hat{a}^\dagger, a)e^{-H(\hat{a}^\dagger, a)t}|\psi\rangle,$$

where operators are assumed to be normal ordered. For simplicity we choose an initial state,  $|\psi\rangle = \sum_n P_n (\hat{a}^\dagger)^n |0\rangle$ , with  $P_n = e^{-1}/n!$ , thus  $|\psi\rangle = e^{\hat{a}^\dagger - 1} |0\rangle$ . Since we are interested in properties which are independent of the precise form of the initial condition, this particular choice does not have an important effect.

From (15) and general properties of the propagator it follows that

$$\langle \hat{Q}(t) \rangle = \langle 0|Q(1, \hat{a}) \times \left[ e^{-H(\hat{a}^\dagger + 1, a)\Delta t} \dots e^{-H(\hat{a}^\dagger + 1, a)\Delta t} \right] e^{\hat{a}^\dagger} |0\rangle,$$

where the square brackets contain a product of  $N$  infinitesimal propagators for times  $\Delta t = t/N$ . Now, we insert  $N + 1$  identity operators (17) between the various terms of the above product. Using (16) and taking the continuum limit,  $N \rightarrow \infty$ ,

we obtain the expectation value  $\langle Q(t) \rangle$  in the form of a path integral

$$\langle Q(t) \rangle = \int \mathcal{D}[a^*, a] e^{-F_0} Q(1, a(t)) e^{-|a(0)|^2 + a^*(0)}$$

where  $F_0$  is the action of the system

$$F_0 = \int_0^t d\tau \{a^*(\tau) \partial_\tau a(\tau) + H[a^*(\tau) + 1, a(\tau)]\},$$

and  $\mathcal{D}[a^*, a] = \prod_\tau [d^2a(\tau)/\pi]$  is the measure of the integral.

Having the path integral expression for the propagator, the generalization to the finite dimensional case is straightforward. It merely amount for the addition of a diffusive term in the action. Thus the action of the diffusion-reaction process (1) is

$$F = \int d\mathbf{r} d\tau \left\{ a^*(\partial_\tau - D\nabla^2) a + \frac{\mu}{2} [a^{*2} a^2 - 2a^* a^2] \right\},$$

where, now,  $a^*(r, \tau)$  and  $a(r, \tau)$  are functions of the time  $\tau$  as well as the space coordinates  $\mathbf{r}$ . Henceforth we omit the explicit time and space dependence of the fields.

The action associated with the Lotka-Volterra process (3) can be derived in the same way, and the result is:

$$F = \int a^*(\partial_\tau - D\nabla^2) a + b^*(\partial_\tau - D\nabla^2) b + \tilde{H}, \quad (18)$$

where

$$\tilde{H} = \mu a^* a - \sigma(1 + b^*) b^* b + \lambda(a^* + 1)(b^* - a^*) ab.$$

Finally we remark that, unlike quantum mechanics of many-body bosons where fields are periodic in imaginary time, here there are no such boundary conditions.

## 6. The mean field equations

The mean field equations of the field theory defined by the action (18) are the saddle point equations of the bare action,

$$\delta F = 0,$$

where the functional derivative is with respect to all the fields,  $a$ ,  $a^*$ ,  $b$  and  $b^*$ . Seeking for a

solution with non vanishing densities  $\bar{n}_A = \langle \hat{a} \rangle$ ,  $\bar{n}_B = \langle \hat{b} \rangle$ , the saddle fields (which we denote by bar) are  $\bar{a}^* = \bar{b}^* = 0$ , and solutions of the equations

$$\begin{aligned}\frac{d\bar{a}}{d\tau} &= D\nabla^2\bar{a} - \mu\bar{a} + \lambda\bar{a}\bar{b}, \\ \frac{d\bar{b}}{d\tau} &= D\nabla^2\bar{b} + \sigma\bar{b} - \lambda\bar{a}\bar{b}.\end{aligned}$$

Thus the mean filed equations of the quantized Lotka-Volterra system are precisely the Lotka-Volterra equations (4).

The steady state solutions of (4),  $dn_A/dt = dn_B/dt = 0$ , admit only homogeneous densities in space [8]. They are associated with the fixed-points of the equations: One is the unstable hyperbolic fixed-point,  $n_A = n_B = 0$ , corresponding to the case with no reactants in the system. The second,  $n_A = 0$ ,  $n_B = \infty$ , represents the situation where the number of prey grows indefinitely in the absence of predator. The third fixed-point,  $\bar{n}_A = \sigma/\lambda$ ,  $\bar{n}_B = \mu/\lambda$ , is an elliptic fixed-point corresponding to a balanced ecological state with fixed populations. Linearizing equations (4) around the latter fixed-point we obtain:

$$\frac{d}{dt} \begin{pmatrix} \Delta n_A \\ \Delta n_B \end{pmatrix} \simeq -M_0 \begin{pmatrix} \Delta n_A \\ \Delta n_B \end{pmatrix}, \quad (19)$$

where

$$M_0 = \begin{pmatrix} 0 & -\sigma \\ \mu & 0 \end{pmatrix}, \quad (20)$$

$$\Delta n_A = n_A - \bar{n}_A, \text{ and } \Delta n_B = n_B - \bar{n}_B.$$

The matrix  $M_0$ , which we shall call the bare mass matrix, is the generator of time evolution of homogeneous densities in the vicinity of the fixed-point. Its eigenvalues determine the stability properties of the fixed-point. If the real parts of the eigenvalues are positive, the fixed-point is stable, while if negative, it is unstable. In our case, the eigenvalues of  $M_0$  are purely imaginary,  $\epsilon_{\pm} = \pm i\sqrt{\mu\sigma}$ . It implies that close enough to the fixed-point the population densities oscillate in time. Moreover, a nonlinear stability analysis of the Lotka-Volterra equations shows that the system exhibits periodic evolution over the whole phase space. The reason is the existence of a con-

served quantity[1] (for homogeneous densities),

$$K = n_A + n_B - \frac{\mu}{\lambda} \ln(n_B) - \frac{\sigma}{\lambda} \ln(n_A), \quad (21)$$

which confines the phase space trajectories to move along concentric closed loops, as shown in Fig. 1.

Notice that elliptic fixed-points are unstable with respect to small perturbations. Any small perturbation might shift the eigenvalues  $\epsilon_{\pm}$  off the imaginary axis. Consequently the elliptic fix-point will become either a stable or an unstable focus. In what follows it will be shown that discretization effects, which lie beyond the mean field description, indeed, lead to such a scenario.

## 7. Renormalization procedure

An effective action of a filed theory is obtained by integrating out the “fast” degrees of freedom. The procedure is usual: First, we separate the fields into “fast” and “slow” components. Say for the annihilation process (1),  $a = a_f + a_s$ , where  $a_f$  and  $a_s$  denote Fourier components of the field which oscillate rapidly or slowly in space, respectively. Next, we expand the action  $F[a, a^*]$  up to second order in the fast fields:  $F \simeq F[a_s, a_s^*] + F_2[a_s, a_s^*; a_f, a_f^*]$ , where  $F_2$  is quadratic in the fast fields  $a_f$  and  $a_f^*$ . Then the effective action,  $F_{eff}[a_s, a_s^*]$ , is obtained by integrating out the fast fields,

$$e^{-F_{eff}} = \int \mathcal{D}[a_f, a_f^*] e^{-F[a_s, a_s^*] - F_2[a_s, a_s^*, a_f, a_f^*]}.$$

For the binary annihilation reaction, the effective action has been calculated by Cardy and Tauber [7]. From this calculation they prove that, for  $d > 2$ , the mean field equations hold, and the density of reactants decreases as  $n(t) \sim 1/t$ . However, when  $d < 2$ , inherent spatial fluctuations result in a decrease of the asymptotic annihilation rate,  $n(t) \sim 1/t^{d/2}$  [2].

Notice, however, that in the binary annihilation example the fixed-point  $n_A(t \rightarrow \infty) = 0$  does not change due to discretization effects. Only the asymptotic approach to this point alters. As we shall see, in the Lotka-Volterra system the renormalization procedure results in a more dramatic effect. The nature of the fix-point itself

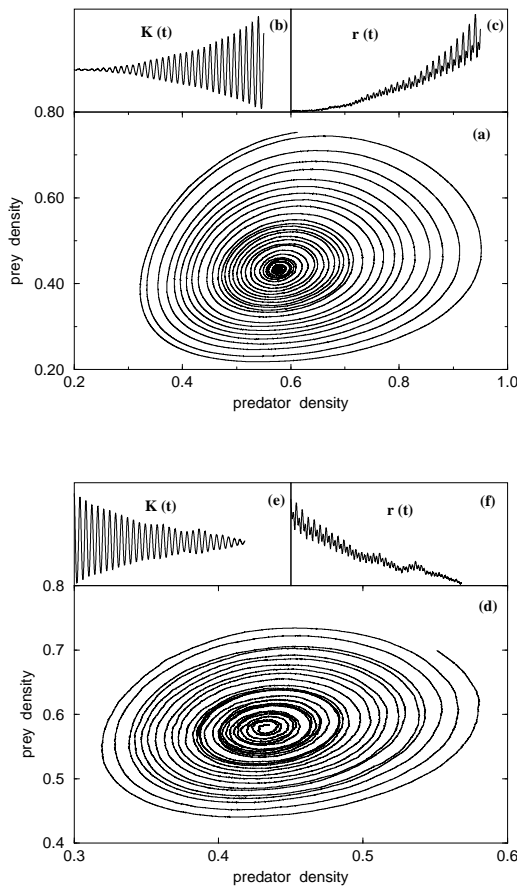


Figure 2. The behavior of the discretized Lotka-Volterra systems in two dimensions. The upper figure shows results calculated for the case  $\sigma > \mu$  where the fixed-point is an unstable focus: (a) The form of a phase space trajectory (tern in time being clockwise); (b) The time dependence of the function  $K(n_A, n_B)$  (Eq. 21); (c) The time dependence of the distance from the center. The lower figure shows, correspondingly, the behavior for  $\mu > \sigma$  where the fixed-point is a stable focus. These figures were obtained by Monte Carlo simulation on a  $1000 \times 1000$  lattice sites with hopping rate  $D = 1$  (where the lattice constant has been set to unity) and  $\lambda = 0.005$ . In the upper panel  $\sigma = 0.0008$  and  $\mu = 0.0006$ , while for the lower one  $\mu = 0.0008$  and  $\sigma = 0.0006$ .

changes. To put it differently, if one associates the long time asymptotic behavior of the system with the ground state of the field theory defined by the action (18), then quantization leads to a new ground state which differ from the “classical” ground state described by the Lotka-Volterra equations (4). Moreover, by changing the parameter  $\mu - \sigma$  the system undergoes a phase transition between distinct ground states, a scenario which is analogous to quantum phase transitions.

In what follows we consider only the physical situation of the critical dimension,  $d = 2$ , and defer the technical details of the derivation of the effective action of the Lotka-Volterra system to the Appendix.

Given the fixed-point of the Lotka-Volterra equations (4) at finite densities,  $(\bar{n}_A, \bar{n}_B) = (\frac{\sigma}{\lambda}, \frac{\mu}{\lambda})$ , it is convenient to change variables to fields which represent fluctuations around this fixed-point, namely,  $a \rightarrow a + \bar{n}_A$ , and  $b \rightarrow b + \bar{n}_B$ . The bare Green function,  $G^0$ , associated with the quadratic part of the resulting action is,

$$G^0 = [(\partial_t - D\nabla^2)\tau_0 + M_0]^{-1}, \quad (22)$$

where  $\tau_0$  is the identity matrix, and  $M_0$  is the bare mass matrix (20). Dyson's equation for the exact Green function,  $G$ , is,

$$G = G^0 + G^0 \Sigma G, \quad (23)$$

where  $\Sigma$  is the self energy. The correction for the mass matrix is the zero Fourier components of the self energy,  $\delta M = \Sigma(k = 0, \omega = 0)$ .

A perturbative calculation (see Appendix) shows that the leading order result for  $\delta M$  is given by:

$$\delta M \simeq 2\lambda S \begin{pmatrix} \mu & \sigma \\ -\mu & -\sigma \end{pmatrix}, \quad (24)$$

where

$$S = \frac{1}{16\pi D} \ln \left( 1 + \frac{D^2 \Lambda^4}{\mu\sigma} \right), \quad (25)$$

$\Lambda$  being the upper momentum cut-off. Diagonalizing the full mass matrix,  $M \simeq M_0 + \delta M$ , we obtain the eigenvalues  $\epsilon_{\pm} \simeq (\mu - \sigma)\lambda S \pm i\sqrt{\mu\sigma}$ , where it was assumed that  $\lambda S \ll 1$ . Evidently, the eigenvalues of the mass matrix acquire a negative

or positive real part depending whether  $\mu < \sigma$  or  $\sigma < \mu$ , respectively. It implies that the elliptic fixed-point becomes an attractive focus in the first case, and a repulsive one in the second. Thus, a change in  $\mu - \sigma$  from a positive to a negative value induces a phase transition in the long time asymptotic behavior of the system. These results are verified by the Monte Carlo simulations shown in Fig. 2.

The small parameter of the above perturbation theory is  $\lambda S \ll 1$ . The nonperturbative regime of our theory is when  $\lambda S > 1$ , or

$$\mu\sigma < D^2\Lambda^4 \exp\left\{-16\pi\frac{D}{\lambda}\right\} \quad (26)$$

In this case one can write a Dyson equation for the mass matrix with logarithmic accuracy. I.e. assuming  $\lambda S \gg 1$  but still  $\lambda/(16\pi D) \ll 1$ , the mass matrix satisfies the equation

$$M = M_0 + M_1(1 - M^{-1}M_1)^{-1}, \quad (27)$$

where

$$M_1 = 2\frac{\lambda S}{1 + \lambda S} \begin{pmatrix} \mu & \sigma \\ -\mu & -\sigma \end{pmatrix}. \quad (28)$$

The above equation is a quadratic equation for the mass matrix which can be easily solved. The physical solution is the one which is continuously related to the perturbative result obtained before. Thus, when  $\lambda S \rightarrow \infty$ , the eigenvalues of the mass matrix are

$$\epsilon_{\pm} = \frac{1}{8} \left[ \alpha(\mu - \sigma) \pm \sqrt{\alpha^2(\mu - \sigma)^2 - \beta\mu\sigma} \right],$$

where  $\alpha = 9 - \sqrt{65}$  and  $\beta = 32(\sqrt{65} - 7)$ . This result shows that, in the strong coupling case, the parameter space of the system breaks into four domains, see Fig. 3: The first,  $\sigma > \mu > \sigma/40.6$ , where the fixed-point is an unstable focus. The second,  $\sigma < \mu < 40.6\sigma$ , where it is an absorbing focus. The third regime is  $\mu > 40.6\sigma$ , where the fixed-point is a stable node, and the forth regime  $\mu < \sigma/40.6$  is characterized by an unstable node.

The critical line  $\mu = \sigma$  is a border line at which the system switches between different ground states. It is natural inquire about the nature of the ground state of the system when the focus becomes unstable. What is the global behavior of

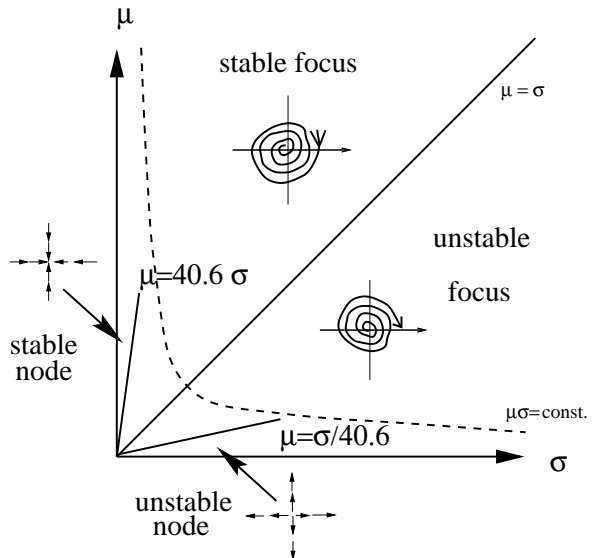


Figure 3. The phase diagram of the discretized Lotka-Volterra system in two dimensions. The dashed line represents the line where the system crosses over from the weak to the strong coupling regime, see Eq. 26. In the weak coupling regime, two cases are identified:  $\mu > \sigma$  corresponding to stable focus, and  $\mu < \sigma$  corresponding to unstable focus. In the strong coupling regime two other regions are developed: A stable node in the range  $\mu < 40.6\sigma$ , and an unstable node when  $\mu < \sigma/40.6$ .

trajectories in phase space when the fixed-point is an unstable focus? There are two sensible scenarios: (a) One of the other mean field fixed-points,  $n_A = n_B = 0$  or  $n_A = 0, n_B = \infty$ , becomes stable due discretization, and all the trajectories converge to this point. (b) Some other type of attractive manifold, such as a limit cycle, if formed. In Fig. 4 we present numerical results for the system in the unstable regime. The behavior of the trajectories indicates that the second scenario takes place.

## 8. Summary

We have shown that the discreteness of the reactants in Lotka-Volterra systems in two di-

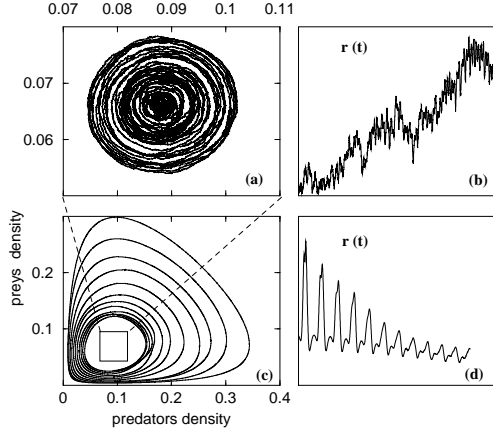


Figure 4. The global behavior of phase space trajectories in case of unstable focus, as obtained for  $D = 1$ ,  $\lambda = 0.01$ ,  $\sigma = 0.0008$  and  $\mu = 0.0006$ . When the initial conditions are near the unstable fixed-point (a), the distance from the fixed-point grows with time (b). Yet, starting far away from the fixed-point (c), the distance decreases (d). This indicate the existence of some attractive manifold similar to a limit cycle.

mensions, results in a behavior (Figs. 2 and 4) which differs from that of the Lotka-Volterra equations (Fig. 1). The parameter space of the rates  $(\sigma, \mu, \lambda)$  breaks into subspaces of distinct behavior (Fig. 3). The transition between these subspaces is analogous to a quantum phase transition between different ground states. Our analysis was limited to a close vicinity of the fixed-point. It showed that as  $\mu - \sigma$  changes sign, from positive to negative, the fixed-point becomes unstable. The numerical simulations (Fig. 4) indicated that this instability signals the formation of a new ground state where an attractive manifold similar to a limit cycle is formed. Further studies on this subject will be focused on the nature of the unstable phase, and behavior of the system in one dimension.

## 9. Appendix

In this appendix we provide some details of the renormalization procedure for the Lotka-Volterra system. Our discussion will be limited to properties of the system near the fixed-point. It is therefore convenient to change variables to fields which describe fluctuations around this fixed-point. Thus changing variables as  $a \rightarrow a + \bar{n}_A$ ,  $b \rightarrow b + \bar{n}_B$ , the action (18) takes the form

$$F = \int dr dt a^* (\partial_t - D \nabla^2) a + b^* (\partial_t - D \nabla^2) b + \bar{H},$$

where

$$\begin{aligned} \bar{H} = & \mu b^* a - \sigma a^* b + \sigma (a^* - b^*) b^* b - \sigma a^* a^* b \\ & + \mu (b^* - a^*) a^* a + \lambda (b^* - a^*) b a + \lambda a^* a b^* b \\ & - \lambda a^* a^* a b + \frac{\mu \sigma}{\lambda} (b^* a^* - a^* a^* - b^* b^*). \end{aligned}$$

To construct the quadratic part of the action in the fast variables,  $F_2$ , it is convenient to represent the fields in terms of their Fourier components, e.g.  $a(\mathbf{k}, \omega) = \int dt dr e^{i\mathbf{k} \cdot \mathbf{r} + i\omega t} a(\mathbf{r}, t)$ . Now, we define a vector of fast variables  $\Psi_f = (a_f, b_f, a_f^*, b_f^*)^T$ , where the fast fields contain terms only with high values of the momentum  $\mathbf{k}$ . Thus, taking care of causality [7] we have

$$F_2 = \frac{1}{2} \int \frac{d\mathbf{k} d\omega}{(2\pi)^3} \Psi_f^\dagger Z \Psi_f,$$

where elements of the matrix  $Z$  are functions of the slow fields (henceforth we drop the subscript  $s$  of these fields):

$$Z = \begin{pmatrix} G_0^{-1} \tau_0 & \frac{\mu \sigma}{\lambda} (\tau_1 - 2\tau_0) \\ 0 & (G_0^\dagger)^{-1} \tau_0 \end{pmatrix} + z_1 + z_2,$$

$$z_1 = \begin{pmatrix} 0 & (\sigma b + \mu a + \lambda a b) \tau_1 \\ \lambda (b^* - a^*) (1 + a^*) \tau_1 & 0 \end{pmatrix},$$

and

$$z_2 = \begin{pmatrix} 0 & -2\sigma b \tau_0 - (\mu a + \lambda a b) (\tau_0 + \tau_3) \\ 0 & 0 \end{pmatrix}.$$

Here  $G_0$  is the bare Green function of the problem (22),  $\tau_0$  is the identity matrix, and  $\tau_i$  (with  $i = 1, 2, 3$ ) denote the Pauli matrices, where in particular

$$\tau_1 = \begin{pmatrix} 0 & 1 \\ 1 & 0 \end{pmatrix}, \quad \text{and} \quad \tau_3 = \begin{pmatrix} 1 & 0 \\ 0 & -1 \end{pmatrix}.$$

The integration over the fast variables yields  $(\text{Det}Z)^{-1/2}$  which can be written as  $\exp\{-\frac{1}{2}\text{Tr} \ln Z\}$ . Thus the effective action takes the form:

$$F_{eff} = F - \frac{1}{2}\text{Tr} \ln g_0^{-1} - \frac{1}{2}\text{Tr} \ln[1 + g_0(z_1 + z_2)] \quad (29)$$

where

$$g_0 = \begin{pmatrix} G_0\tau_0 & -\frac{\mu\sigma}{\lambda}G_0(\tau_1 - 2\tau_0)G_0^\dagger \\ 0 & G_0^\dagger\tau_0 \end{pmatrix}.$$

It can be shown that the leading contribution comes from the matrix  $z_1$ . Thus neglecting  $z_2$  and expanding the logarithm (29) to second order yields

$$-\frac{1}{2}\text{Tr} \ln[1 + g_0 z_1] \simeq [\mu\sigma + \lambda(\sigma b + \mu a + \lambda ab)] \times (b^* - a^*)(1 + a^*)\delta S$$

where

$$\delta S = \frac{1}{2}\text{Tr} \left\{ G_0\tau_1 G_0^\dagger\tau_1 \right\} = \frac{dl}{8\pi D}.$$

Here the trace is over a momentum shell near the ultraviolet cut-off  $\Lambda$ . Thus  $dl = \ln(\Lambda/\Lambda')$ , where  $\Lambda' = e^{-dl}\Lambda$  is the lower limit of the momentum integral.

In the first approximation for the effective action, one sets  $\Lambda'$  to be the natural lower momentum cut off, which in our case implies that  $\delta S \rightarrow S$ , where  $S$  is given by (25). This is referred as the “perturbative” calculation of the effective action which holds when  $\lambda S \ll 1$ . In the full one-loop renormalization procedure, the above process is repeated an infinite number of times, where in each step the lower momentum cut off is decreased by an infinitesimal amount. The result applies also when  $\lambda S > 1$ , provided  $\lambda/16\pi D \ll 1$  (the condition which allowed us to neglect  $z_2$ ).

The renormalization procedure results in several effects. One is a shift of the fixed-point  $\bar{n}_A, \bar{n}_B$ . This is due to the appearance of terms linear in  $a^*$  and  $b^*$ . The second effect is a change of the mass matrix and its eigenvalues. This is the most interesting effect since it determined the stability of the fixed-point. Finally we have a renormalization of the coupling constant  $\lambda$ .

The renormalization group equation for  $\lambda$ , in two dimensions, takes the form:

$$\frac{d\lambda}{dl} = -\frac{\lambda^2}{8\pi D}.$$

Thus the renormalized value of  $\lambda$  is

$$\lambda_R = \frac{\lambda}{1 + \lambda S}$$

where  $S$  is given by (25). We see that  $\lambda$  flows into the weak coupling limit.

The renormalization equations for the mass matrix are

$$\frac{dM}{dl} = -\frac{\lambda}{4\pi D} \begin{pmatrix} \mu & \sigma \\ -\mu & -\sigma \end{pmatrix},$$

with the initial condition  $M(l = 0) = M_0$ , where  $M_0$  is the bare mass matrix (20). This equation can be easily integrated. The result is  $M \simeq M_0 + M_1$  where  $M_1$  is given by (28). A self consistent Dyson equation which takes into account higher order corrections to the mass matrix takes the form (27). This self consistent approximation is analogous to the self consistent Born approximation in disorder physics which includes the “rainbow diagrams”.

## REFERENCES

1. See, e.g., J. D. Murray, *Mathematical Biology* (Springer-Verlag, N.Y., 1993) and references therein.
2. D. Toussaint and F. Wilczek, *J. Chem. Phys.* **78**, 2642 (1983).
3. A. A. Ovchinnikov and Ya. B. Zeldovich, *Chem. Phys.* **28**, 215 (1978).
4. A. J. Lotka, *Proc. Natl. Acad. Sci. USA* **6**, 410 (1920).
5. V. Volterra, *Lecon sur la Theorie Mathematique de la Lutte pour le via* (Gauthier-Villars, Paris, 1931).
6. M. Doi, *J. Phys. A* **9**, 1465 (1976); L. Peliti, *J. Physique* **46**, 1469 (1985); B. P. Lee, *J. Phys. A* **27** 2633 (1994);
7. J. Cardy and U. C. Tauber, *Phys. Rev Lett.* **77**, 4780 (1996).
8. A. Okubo, *Diffusion and Ecological Problems: Mathematical Models* (Springer-Verlag, N.Y., 1980).